Thermal and Mechanical Characterization of Linear Low-Density Polyethylene/Wood Flour Composites

Norma E. Marcovich,[1] Marcelo A. Villar[2]

[1]*Instituto de Investigaciones en Ciencia y Tecnologia de Materiales (INTEMA), Facultad de Ingeniería, Universidad Nacional de Mar del Plata, Juan B. Justo 4302, 7600 Mar del Plata, Argentina*
[2]*Planta Piloto de Ingeniería Química, Planta Piloto de Ingeniería Química (Universidad Nacional del Sur-Consejo Nacional de Investigaciones Científicas y Técnicas), Camino "La Carrindanga" Km. 7, 8000 Bahía Blanca, Argentina*

Received 18 October 2002; accepted 11 March 2003

ABSTRACT: A linear low-density polyethylene (LLDPE) matrix was modified with an organic peroxide and by a reaction with maleic anhydride (MAn) and was simultaneously compounded with untreated wood flour in a twin-screw extruder. The thermal and mechanical properties of the modified LLDPE and the resulting composites were evaluated. The degree of crystallinity was reduced in the modified LLDPE, but it increased with the addition of wood flour for the formation of the composites. Significant improvements in the tensile strength, ductility, and creep resistance were obtained for the MAn-modified composites. This enhancement in the mechanical behavior could be attributed to an improvement in the compatibility between the filler and the matrix. © 2003 Wiley Periodicals, Inc. J Appl Polym Sci 90: 2775–2784, 2003

Key words: composites; thermal properties; mechanical properties; compatibilization

INTRODUCTION

Composites based on thermoplastic resins are now becoming popular because of their processing advantages.[1] Nowadays, many inorganic fillers, including talc, mica, clay, glass fiber, and calcium carbonate, are being incorporated into thermoplastics. Nevertheless, organic fillers have drawn attention because of their abundant availability, low cost, and renewable nature. In recent years, cellulosic fillers have attracted considerable interest for the reinforcement of thermoplastics such as polypropylene, polyethylene (PE), and polystyrene, which melt or soften at relatively low temperatures.[2] Among organic fillers, wood and cellulose fibers offer a number of benefits as reinforcements for synthetic polymers because they have a high specific strength and stiffness,[3] a low hardness, which minimizes the abrasion of the equipment during processing, a relatively low density, biodegradability, and a low cost on a unit volume basis.[4–6] Finally, bulk composites made from polyolefins and cellulosic fillers may eventually be recycled or burned to recover heat, without the production of residues or toxic byproducts.[7]

Contrary to many thermoplastic polymers, cellulosic fillers are predominantly polar because of the presence of polar groups on the different components and thus easily absorb moisture. Other important drawbacks of these cellulosic materials in thermoplastic composites include the thermal instability of the fibers at the typical processing temperatures of thermoplastics (around 200°C and higher), the poor interfacial adhesion between the filler and matrix, and the poor fiber dispersion.[6] Thus, the development of methods for controlling the interfacial adhesion between chemically and physically incompatible phases has been the object of considerable efforts.[8] Several techniques, ranging from grafting short-chain molecules onto fiber surfaces to using coupling/adhesion promoting agents, have been reported.[8–12]

In this study, a linear low-density polyethylene (LLDPE) matrix was modified with an organic peroxide and by a reaction with maleic anhydride (MAn) and was simultaneously compounded with untreated wood flour. The thermal and mechanical properties of the resulting LLDPE/wood flour composites were studied. The fracture surfaces of the composite samples, at the temperature of liquid nitrogen, were observed with scanning electron microscopy (SEM).

MATHEMATICAL APPROACH

Young's modulus

The random distribution of the constituent phases in a filled system demands a statistical approach, but this

Correspondence to: N. E. Marcovich (marcovic@fi.mdp.edu.ar).

Contract grant sponsor: National Research Council of República Argentina.
Contract grant sponsor: Antorchas Foundation.

requires the knowledge of the distributions of the different phases. Consequently, the problem can be simplified with a two-phase model in which average stresses and strains are considered to exist in each phase.[13] Among others, models proposed by Takayanagi[14] can be used to predict Young's modulus of composites. For a dispersed phase (filler) in a matrix (polymer), there are two limits for the stress transfer. For efficient stress transfer perpendicular to the direction of the tensile stress, a series–parallel model has been postulated. In this case, the overall modulus is given by the contribution of two components in parallel (the entire dispersed phase and part of the continuous phase) and in series with the contribution of the remaining continuous phase:

$$\frac{1}{E_c} = \frac{\phi}{\lambda E_f + (1 - \lambda)E_m} + \frac{1 - \phi}{E_m} \quad (1)$$

If the stress transfer across planes containing the tensile stress is weak, a parallel–series model is appropriate. In this case, the continuous phase combines in series with the entire dispersed phase before combining in parallel with the remaining continuous phase, giving a modulus:

$$E_c = \lambda\left(\frac{\phi}{E_f} + \frac{1 - \phi}{E_m}\right)^{-1} + (1 - \lambda)E_m \quad (2)$$

In both models, E_m and E_f are the moduli of the matrix and fiber, respectively; E_c is the modulus of the composite; λ is the volume fraction of the series element; and ϕ is an adjustable parameter that can be related to the morphology of the composite. If the fibers are purely elastic, the volume fraction of the fibers (V_f) becomes

$$V_f = \lambda\phi \quad (3)$$

Introducing eq. (3) into eqs. (1) and (2), we obtain the following expressions:

$$\frac{1}{E_c} = \frac{1}{V_f E_f + (\phi - V_f)E_m} + \frac{1 - \phi}{E_m} \quad (4)$$

$$E_c = E_m\left(1 - \frac{V_f}{\phi}\right) + \left(\frac{V_f E_m E_f}{E_m\phi^2 + (1 - \phi)\phi E_f}\right) \quad (5)$$

Creep behavior

Few problems in viscoelasticity can be solved with the Maxwell or Kelvin elements alone, and more often they are used together or in combination. The four-element model is the combination of the Maxwell element and the Kelvin element in series. It is the simplest model that exhibits all the essential features of viscoelasticity[15] and is widely used to model creep behavior. When a constant load is applied, the initial deformation comes from the single spring with modulus E_1. Later deformation comes from the spring with modulus E_2 and the dashpot with viscosity η_2 in parallel and from the dashpot with the viscosity η_1. The total deformation of the model is the sum of the individual deformations of the three parts, as shown in the following expression:

$$\varepsilon(t) = \frac{\sigma_0}{E_1} + \frac{\sigma_0}{E_2}\left[1 - \exp\left(-t\frac{E_2}{\eta_2}\right)\right] + t\frac{\sigma_0}{\eta_1} \quad (6)$$

where σ_0 is the applied stress and t is the creep time.

EXPERIMENTAL

Materials

Wood flour from *Eucalyptus saligna* (Argentina) was used as a reinforcing filler. Only particles that could pass through a 100-mesh sieve (Tyler series) were used in this study, and so the maximum particle average diameter was 147 μm. The polymeric matrix was LLDPE (weight-average molecular weight $\approx$ 120,000), which was kindly provided by Dow–Polisur (Bahía Blanca, Argentina).

PE was chemically modified with MAn (Maleic S.A., La Plata, Argentina), with 2,5-dimethyl 2,5-diterbuthyl-peroxyhexane (DBPH; Petroquímica Cuyo S.A.I.C., Mendoza, Argentina) used as an initiator. For comparison, samples modified only with DBPH were also prepared. The composites and PE modifications were carried out in a Göttfert counterrotating twin-screw extruder 35 mm in diameter with a length/diameter ratio of 15:1 (Buchen, Germany). The temperature of the barrel was controlled in its five sections with the following profile: 120 (feeding zone), 180, 190, 180, and 220°C (die). The extruded melt was cooled and pelletized. The materials obtained were then hot-pressed in a 180 mm $\times$ 180 mm mold at 38 kg/cm^2 and 140°C for 20 min; this was followed by slow cooling. The applied pressure was also maintained during the cooling step. The thickness of the plaques was controlled to approximately 3 mm. The characteristics of the modified polymers and composites and the nomenclature used in this article are reported in Table I.

Physical and mechanical tests

The thermal characterization of the materials was carried out with a differential scanning calorimetry (DSC) instrument (PerkinElmer Pyris 1, Norwalk, CT) equipped with an ice/water bath as a cooling unit and operating under a nitrogen atmosphere (20 mL/min). All the samples were subjected to the same thermal

TABLE I
Nomenclature and Composition of PEs and Wood Flour Composites

Material	LLDPE (wt %)	Wood flour (wt %)	MAn (wt %)	Peroxide[a]
PE	100	0	—	No
PEP	100	0	—	Yes
PEPM	99	0	1	Yes
PEA-30	70	30	—	No
PEAP-30	70	30	—	Yes
PEAM-30	69.5	29.8	0.7	Yes
PEA-40	60	40	—	No
PEAP-40	60	40	—	Yes
PEAM-40	59.6	39.8	0.6	Yes

[a] 0.05 wt % peroxide (DBPH) with respect to LLDPE was used in all cases.

history: they were heated at 10°C/min from 30 to 180°C, kept at this temperature for 5 min to erase the thermal history, and then cooled down to 30°C at 10°C/min. Finally, the samples were heated from 30 to 180°C at 10°C/min. The melting temperature (T_m) and the heat of fusion (ΔH_m) were calculated from the thermograms obtained during the second heating. The values of ΔH_m were used to estimate the degree of crystallinity [X_c (%)] of each material, with 288.7 J/g taken as the value of the enthalpy of fusion of completely crystalline PE.[16] X_c of the composites was corrected taking into account the wood flour concentration [X_c^{corr} (%)].

Thermogravimetric tests were performed with a Seiko Instruments SII Exstar 6000 thermogravimetric analyzer (Chiba, Japan). Dynamic measurements were carried out in a nitrogen atmosphere from room temperature to 500°C at a heating rate of 10°C/min.

The composites were fractured in liquid nitrogen, and their surfaces were observed by SEM with a JEOL 35 CF microscope (Akishima, Japan). The surfaces were previously coated with gold to avoid charging under the electron beam.

Tensile tests were performed according to ASTM Standard D 638-90 (sample type I, 3 mm thick) with an Instron 8501 universal testing machine at a crosshead speed of 5 mm/min (Buckinghamshire, UK). Young's tensile modulus (E), the yield tensile strength (σ_y), and the elongation at break (ϵ_b) were determined from the stress–strain curves. At least five specimens of each sample were tested.

The Izod impact strength was measured at room temperature with a Fractovis–Ceast impact tester (Torino, Italy) according to ASTM Standard D 256M with notched samples. At least 10 specimens of each composite were tested to obtain the impact strength.

A PerkinElmer DMA 7 dynamic mechanical analyzer was used in creep experiments to measure the deformation as a function of time. The tests were carried out with three-point bending geometry with a specimen platform 15 mm long. The applied static stress was 3.2 MPa, and the temperature was fixed at 50°C.

RESULTS AND DISCUSSION

Thermal characterization

Table II lists T_m, ΔH_m, X_c (%), and X_c^{corr} (%) for the neat polymers and composites. There is a slight decrease in X_c of PE because of the different modifications. The use of an organic peroxide induces the formation of oxy radicals, which abstract hydrogen atoms from the macromolecules, generating macroradicals that mostly participate in combination reactions producing chain linking, such as crosslinking, long-chain branching, and chain extension.[17] However, it is known that PE reacts with MAn in the presence of peroxide catalysts to form maleated PE.[11] In similar studies, it has been argued[18] that the grafting of diethylmaleate onto LLDPE occurs preferentially in the secondary carbons of LLDPE, thereby interrupting the linear crystallizable sequences of the polymer. Thus, both modifications contribute to decreasing the initial order of the PE molecules, and X_c consequently decreases.

A slight increment in X_c with the increment of the filler content in the composites has also been observed. The higher X_c value of the composites indicates that the crystallization process is favored by the presence of wood flour particles. This effect is attributed to the nucleation effect of the wood flour: the fibers act as sites for heterogeneous nucleation that induce the crystallization of the matrix. This increase in X_c is exhibited by all the composites, and so it is thought to be independent of the degree of compatibility between the matrix and the filler.

The thermal degradation of thermoplastics occurs by three primary mechanisms: random scission, depolymerization, and degradation involving thermally labile defects or weak links. However, degradation is usually a complex process involving combinations of these mechanisms. The initiation of degradation often

TABLE II
Thermal Characterization of PEs and Wood Flour Composites

Sample	T_m (°C)	ΔH_m (J/g)	X_c (%)	X_c^{corr} (%)
PE	122.2 ± 0.1	111.3 ± 0.6	38.5 ± 0.2	38.5 ± 0.2
PEP	121.9 ± 0.1	107.3 ± 0.5	37.1 ± 0.2	37.1 ± 0.2
PEPM	120.7 ± 0.7	103.0 ± 1.6	35.7 ± 0.6	35.7 ± 0.6
PEA-30	122.3 ± 0.2	81.0 ± 1.5	28.1 ± 0.5	40.1 ± 0.7
PEAP-30	122.3 ± 0.1	79.1 ± 0.9	27.4 ± 0.3	39.2 ± 0.4
PEAM-30	122.2 ± 0.4	77.4 ± 1.8	26.8 ± 0.6	38.6 ± 0.8
PEA-40	122.3 ± 0.1	70.5 ± 2.2	24.5 ± 0.8	40.8 ± 1.2
PEAP-40	122.4 ± 0.3	70.2 ± 0.5	24.3 ± 0.1	40.5 ± 0.1
PEAM-40	121.9 ± 0.1	67.9 ± 1.2	23.5 ± 0.4	39.5 ± 0.7

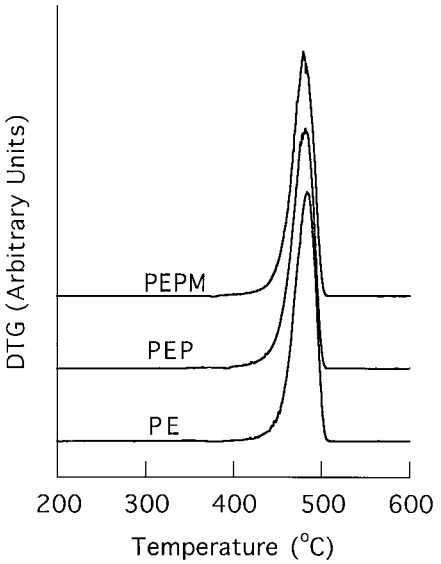

Figure 1 Derivative thermogravimetry curves of unmodified PE and modified PEs (PEP and PEPM).

occurs at thermally labile groups within the polymer chain or terminal to it. Typical commercial polymers contain chemically incorporated impurities. Specifically, in PE, oxygen (ether and peroxide), unsaturations, and branch points are such weak links. The thermooxidative degradation of PE is an autocatalytic process, being a free-radical reaction with degenerate chain branching.[19] Figure 1 shows the result of thermogravimetry tests (derivative thermogravimetry curves) performed on the different PEs. The curves have been vertically shifted to facilitate the comparison. Although all the samples degrade in the same range of temperatures, the temperature at which the high rate of degradation occurs is slightly lower for the modified PEs (479 and 482°C for PE modified by the addition of 0.05 wt % of peroxide (PEP) and PE modified by the addition of 0.05 wt % of peroxide and 1 wt % of maleic anhydride (PEPM), respectively) than for the original PE (484°C). This behavior was expected because an organic peroxide was incorporated to obtain the modified PEs and so those polymers contained more weak links than the neat PE.

Thermal degradation is a crucial aspect in the development of natural fiber composites because it strongly affects the maximum temperature used in the processing of the composites.[20] Figure 2 shows the thermal degradation patterns of PE, PEA-30, PEA-40, and neat wood flour. Below 100°C, a 6 wt % weight loss can be observed in the wood flour curve, which can be attributed to moisture lost from the fibers. Further thermal degradation appears to take place as a two-step process. For untreated woods, noncombustible products, such as carbon dioxide, traces of inorganic compounds, and water vapor, are produced between 100 and 200°C. At about 175°C, some components begin to decompose chemically: low-temperature degradation at a low rate occurs in lignin and hemicelluloses.[21] Major weight loss takes place during the second step of thermal degradation and may be due to the thermal depolymerization of hemicellulose and the cleavage of the glucosidic linkage of cellulose.[22] It has also been associated with the pyrolytic degradation of lignins, involving the fragmentation of interunit linkages (releasing monomeric phenols into the vapor phase), decomposition, and the condensation of aromatic rings.[23] Above 450°C, the lignin component contributes to char formation, and the charred layer helps to insulate the material from further thermal degradation. The char yield of wood flour is about 20 wt % with respect to the initial sample weight.

Neat PE is stable below 420°C. At higher temperatures, the sample undergoes a one-step degradation process, which ends above 510°C with almost no residue (char yield = 2.5%). The weight loss in the composites begins at lower temperatures (ca. 240°C) than that of pure PE, and the char yields are greater, about 9 and 10% with respect to the initial weight for PEA-30 and PEA-40, respectively. Composites degrade in a three-step process, with the first two corresponding to those of wood flour (the same temperature range) and the third one to PE degradation. As expected, the area of the first two peaks in the differential thermogravimetry curves increases with the wood flour content, whereas the area of the third peak decreases with it. As previously reported for similar systems,[21] no evidence of thermal interactions between the wood flour and PE has been found, and the residual char increases as the filler content increases.

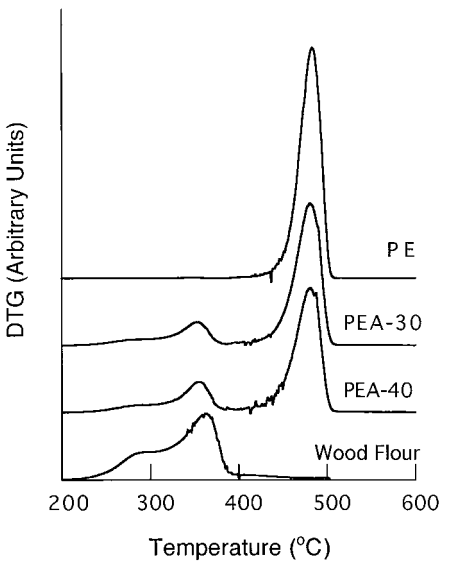

Figure 2 Derivative thermogravimetry curves of PE, PEA-30, PEA-40, and neat wood flour.

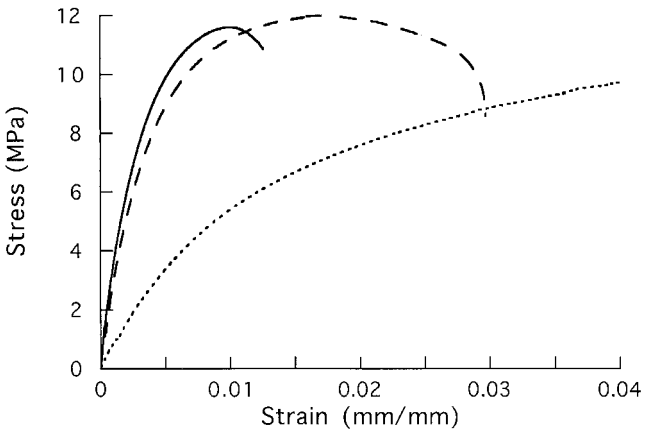

Figure 3 Tensile stress–strain curves of (–) PE, (– – –) PEA-30, and (—) PEA-40.

Mechanical properties

Typical tensile stress–strain curves for PE and PEA composites are shown in Figure 3. Unmodified PE can be elongated more than 35% without fracturing, showing the typical characteristics of ductile polymers: stress whitening followed by necking and drawing with strain hardening after yielding. However, with the addition of wood flour, a ductile to quasibrittle fracture transition occurs, even though a truly brittle behavior has not been observed in the range of concentrations studied. Similar curves (not shown) have also been obtained for a composite prepared from PE modified by the addition of 0.05 wt % of peroxide (PEP) and wood flour (PEAP) and a composite prepared from PE modified by the addition of 0.05 wt % of peroxide and 1 wt % of maleic anhydride (PEPM) and wood flour (PEAM) samples.

Table III illustrates the effects of the wood flour concentration and matrix modification on the tensile properties of the composites. In all cases, the modulus increases with the wood flour content, but the increment is larger for PEA samples. This is the expected behavior because it is well known that the modulus of a filled system depends on the properties of both components, the filler and the matrix. Thus, the modulus of the wood flour being higher than the modulus of PE, the moduli of the filled composites are higher than that of the neat polymer. For example, Woodhams et al.[24] suggested that Young's modulus of wood fibers varies between 10 and 80 GPa; Rohatgi et al.[25] selected 40 GPa as Young's modulus of Kraft wood fibers, and Buttrey[26] suggested 4.9–14 GPa for wood flour. However, the moduli of the PEAM-30 and PEAM-40 composites are higher than those of the PEAP-30 and PEAP-40 composites, respectively, despite the modulus of PEAM being lower than that of PEAP. Hence, as the wood flour used in both composites is the same, this increase in the tensile modulus can be explained by an increased compatibility between the filler and the matrix. The dispersion of the wood flour in the PE matrix is consequently improved by matrix modification, and so the reinforcing effect of the wood flour is more effective than that found for PEAP. It is also known that strong interactions can cause a stiffening effect on the polymer matrix adjacent to the filler particle interphase.[27]

TABLE III
Tensile Properties of PEs and Wood Flour Composites

Sample	E (GPa)	σ_y (MPa)	ε_b (mm/mm)
PE	1.21 ± 0.03	10.58 ± 0.28	> 0.3
PEP	1.00 ± 0.13	9.84 ± 0.16	> 0.3
PEPM	0.85 ± 0.07	9.55 ± 0.25	> 0.3
PEA-30	2.81 ± 0.15	11.94 ± 0.42	$0.026 \pm 5.2 \times 10^{-3}$
PEAP-30	2.56 ± 0.19	12.97 ± 0.30	$0.029 \pm 3.6 \times 10^{-3}$
PEAM-30	2.59 ± 0.19	16.86 ± 0.35	$0.134 \pm 3.0 \times 10^{-2}$
PEA-40	3.50 ± 0.01	11.54 ± 0.39	$0.014 \pm 4.2 \times 10^{-3}$
PEAP-40	3.29 ± 0.29	13.77 ± 0.55	$0.018 \pm 3.0 \times 10^{-3}$
PEAM-40	3.35 ± 0.14	16.59 ± 0.20	$0.052 \pm 7.4 \times 10^{-3}$

TABLE IV
Takayanagi Parameters

	Equation(4)		Equation(5)	
Composite	ϕ	R^2	ϕ	R^2
PEA	0.741	0.9461	0.879	0.9998
PEAP	0.761	0.9557	0.899	0.9992
PEAM	0.801	0.9710	0.923	0.9998

Even though phenomenological approaches are not rigorous, they can be used to roughly estimate the effect of the matrix/interface modification in a composite system.[28] Thus, to further investigate the effect of the filler concentration on the composite modulus, we have compared the experimental curves in tensile experiments to the phenomenological approaches derived by Takayanagi.[47] The wood flour weight fractions have been converted into volume fractions, with 920 kg/m^3 taken as the density of the LLDPE matrix (supplier data) and 1530 kg/m^3 (density of the cell wall) taken as the density of the wood flour.[29] The modulus of the wood flour has been taken to be 40 GPa.[25] For all the composites, the dependence of Young's modulus on the wood flour volume fraction has been satisfactory modeled with eq. (5), as indicated by the high R^2 values. The calculated parameters (ϕ) are listed in Table IV. The value of ϕ increases as the level of the matrix modification increases, and this indicates that the filler–matrix interface is stronger, and a more efficient reinforcing effect is obtained. In other words, a higher value of the ϕ parameter suggests that the efficiency of stress transfer from the matrix to the fibers is improved, as pointed out by other researchers.[30] However, eq. (4) fails to describe all systems, and this shows that stress transfer perpendicular to the direction of the tensile stress is not efficient.

The yield stress of the modified PE composites also increases with the wood flour content, whereas a slight decrease has been observed for a PEA-40 sample with respect to PEA-30. For higher wood flour contents, filler particles begin to form aggregates. Direct physical bonds between filler particles are weak and are thus easily broken during tensile loading. This fact could explain the decrease in the yield stress of the PEA composites at high particle contents. The improved dispersion obtained by the chemical modification of the matrix is, however, also responsible for the continuous increase in the yield stress with the wood flour content. The yield stress generally shows a stronger dependence of interfacial adhesion than Young's modulus; for instance, the tensile yield stress is an excellent property to correlate with interfacial interactions in heterogeneous polymer systems.[31]

As a result of filler addition, the ultimate strain decreases as the wood flour content increases because of the decreased deformability of the matrix (restricted by the rigid particles). However, the decrease in ϵ_b is lower for PEAM composites than for PEA and PEAP composites, and this indicates that interface modification also provides an increase in toughness or ductility.

The general improvements in the mechanical properties due to the addition of MAn to the composites indicate that the compatibility between the hydrophilic cellulosic materials and hydrophobic polymer has increased, and MAn acts as a coupling agent. The function of MAn in a PE/cellulose (wood flour) system was explained by Maldas and Kokta.[10] They suggested that, in the presence of an initiator (organic peroxide), PE and cellulose are linked together by means of MAn forming a graft copolymer containing a succinic half-ester bridge between wood particles and PE segments. Then, PE becomes a side chain of the wood. Moreover, the —OH groups of the wood flour also have the ability of forming hydrogen bonds with the —COOH group of the MAn segment. In this way, MAn develops an overlapping interface area between the wood flour and the polymer matrix. In addition, a strong fiber–fiber interaction due to intermolecular hydrogen bonding has also been diluted, and this leads to better dispersion of the wood flour particles. This reaction was also recently confirmed by Balasuriya et al.[11] with DSC and Fourier transform infrared techniques. Furthermore, the long PE chains of PEPM lead to an adaptation of the very different surface energies of the matrix and fiber, and this allows a good wetting of the fibers by the viscous polymer. Thus, better wettability can increase interfacial adhesion by an increased work of adhesion.[32] The chemical bonding between the anhydride and hydroxyl groups causes better stress transfer from the matrix to the fibers, leading to a higher tensile strength.

The increase in the tensile strength of PEAP composites is related to the peroxide-initiated free-radical reactions between PE and the wood fibers. Combining wood particles and PE radicals leads to the grafting of PE onto wood fibers.[33] The possible reaction is the following: PE · + wood · → PE–wood. Thus, better bonding between the fiber and the matrix results in a higher tensile strength because of more efficient stress transfer. Besides, Nogellova et al.[12] reported that crosslinking gives a substantial increase in the mechanical properties of resulting LDPE/wood flour composites. They also confirmed experimentally the formation of covalent bonding between filler fibers and polymer chains.

Impact behavior

The notched Izod impact energy of the composites is reported in Table V. The energy available in the impact machine was not enough to break the PE and modified PE specimens; therefore, those data are not included. Moreover, other authors reported that low-density PE does not break in notched Izod tests,[34,35] whereas values higher than 850 J/m can be found in the literature.[36] Most of the composite samples broke completely (PEA-30, PEA-40, PEAP-40, and PEAM-40) or nearly completely (PEAP-30 and PEAM-30) during the test. A partial break, according to the definition of ASTM D 256, occurs when less than 10% of the cross section remains unbroken.

The toughness of the composites decreases with an increase in the wood flour concentration because a rigid filler has been added to a tough matrix. Although it is well established that crack propagation becomes more difficult in polymeric matrices reinforced with rigid fillers than in the neat matrices,[37] the decrease of the impact strength with the wood flour content could be attributed to the increment in the fiber ends within the body of a short fiber composite. The presence of short fibers means that there are considerable stress concentrations taking place near the fiber ends at which microcracks form and fibers debond from the matrix, even in ductile matrices.[38] These microcracks could cause crack initiation and, therefore, potential composite fractures.[39] The interactions between neighboring fibers constrain the matrix flow significantly,

TABLE V
Izod Impact Energy of Wood Flour Composites

Sample	E (J/m)
PEA-30	32.21 ± 15.57
PEAP-30	42.01 ± 6.36
PEAM-30	73.73 ± 5.37
PEA-40	28.56 ± 4.21
PEAP-40	29.25 ± 6.24
PEAM-40	47.95 ± 8.88

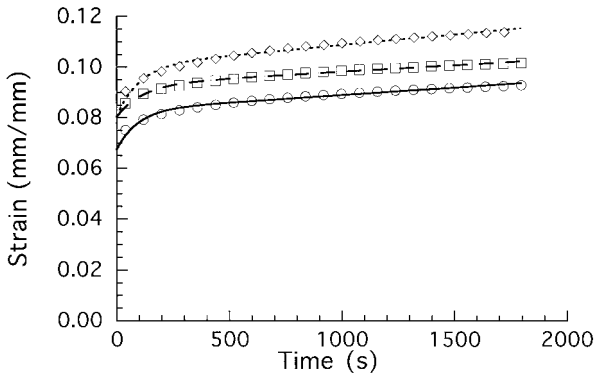

Figure 4 Creep strain as a function of time for PE and modified PE samples: (○,—) PE, (□,– – –) PEP, and (◇,–) PEPM. The symbols represent experimental data, and the lines represent the theoretical model.

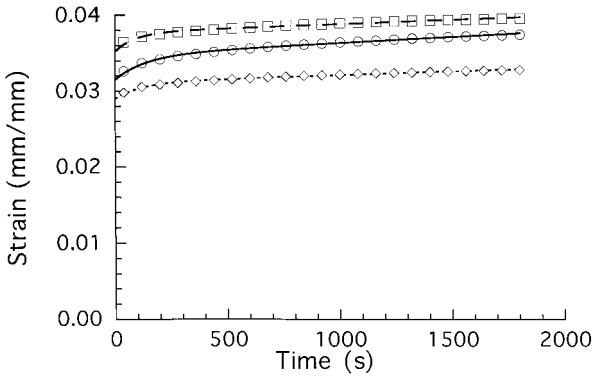

Figure 6 Creep strain as a function of time for composites containing 40 wt % wood flour: (○,—) PEA-40, (□,– – –) PEAP-40, and (◇,–) PEAM-40. The symbols represent experimental data, and the lines represent the theoretical model.

resulting in a deteriorating matrix enbrittlement.[38] Besides, at high filler contents, the probability of fiber agglomeration[40] also increases, and this creates regions of stress concentration that require less energy to initiate or propagate a crack.

However, PEAM samples absorb more energy than other composites, and this is the result of the improved compatibility between the filler and the modified PE. The importance of good adhesion between the fiber and the matrix has long been recognized. Good adhesion between the fibers and the matrix results in efficient stress transfer from the continuous polymer matrix to the dispersed fiber reinforcement and can increase the ability of the material to absorb energy.[8] Oksman and Lindberg,[41] who suggested that, for a higher interfacial adhesion between the matrix and the filler, a higher energy is needed to start crack propagation, reported similar results. In addition, Rana et al.[42] reported that a better fiber–matrix adhesion leads to a better energy absorbing capacity of the composite.

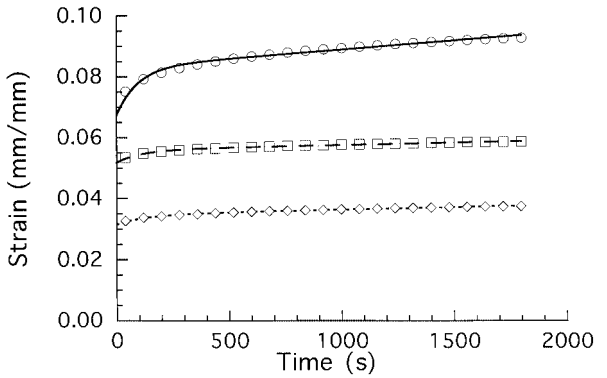

Figure 5 Creep strain as a function of time for PE and PEA samples: (○,—) PE, (□,– – –) PEA-30, and (◇,–) PEPM. The symbols represent experimental data, and the lines represent the theoretical model.

Moreover, because of the polarity of the wood flour, its dispersion in the unmodified PE matrix is poorer than the dispersion of particles in modified PEs, and a tendency toward flocculation and aggregation of the fibers can be expected. These agglomerates are easily broken during an impact test and contribute to the decreased impact strength of PEA samples in comparison with that of PEAM composites. Similar results were reported by Rozman et al.,[43] who studied the mechanical behavior of rubberwood/high-density polyethylene composites.

Short-term creep

Creep in thermoplastics is a complex phenomenon that depends on both material properties (molecular orientation and crystallinity among others) and external parameters (applied stress, temperature, and humidity).[44] The presence of wood fibers introduces several additional parameters that affect the mechanical and creep behavior of composites. These parameters include the fiber volume fraction, fiber aspect ratio, fiber orientation (as a result of the processing), and mechanical properties of the fibers.

TABLE VI
Parameters Derived from Curve Fitting Eq. (6) to Creep Data

Material	$E_1 \times 10^{-7}$ (Pa)	$E_2 \times 10^{-8}$ (Pa)	$\eta_2 \times 10^{-10}$ (Pa s)	$\eta_1 \times 10^{-11}$ (Pa s)
PE	4.745	2.059	1.938	5.304
PEP	3.979	2.549	2.946	6.093
PEPM	3.974	1.609	1.610	3.819
PEA-30	6.178	7.824	8.730	18.88
PEA-40	10.16	9.959	13.84	19.27
PEAP-40	9.088	13.00	11.63	26.96
PEAM-40	11.02	15.54	18.92	30.78

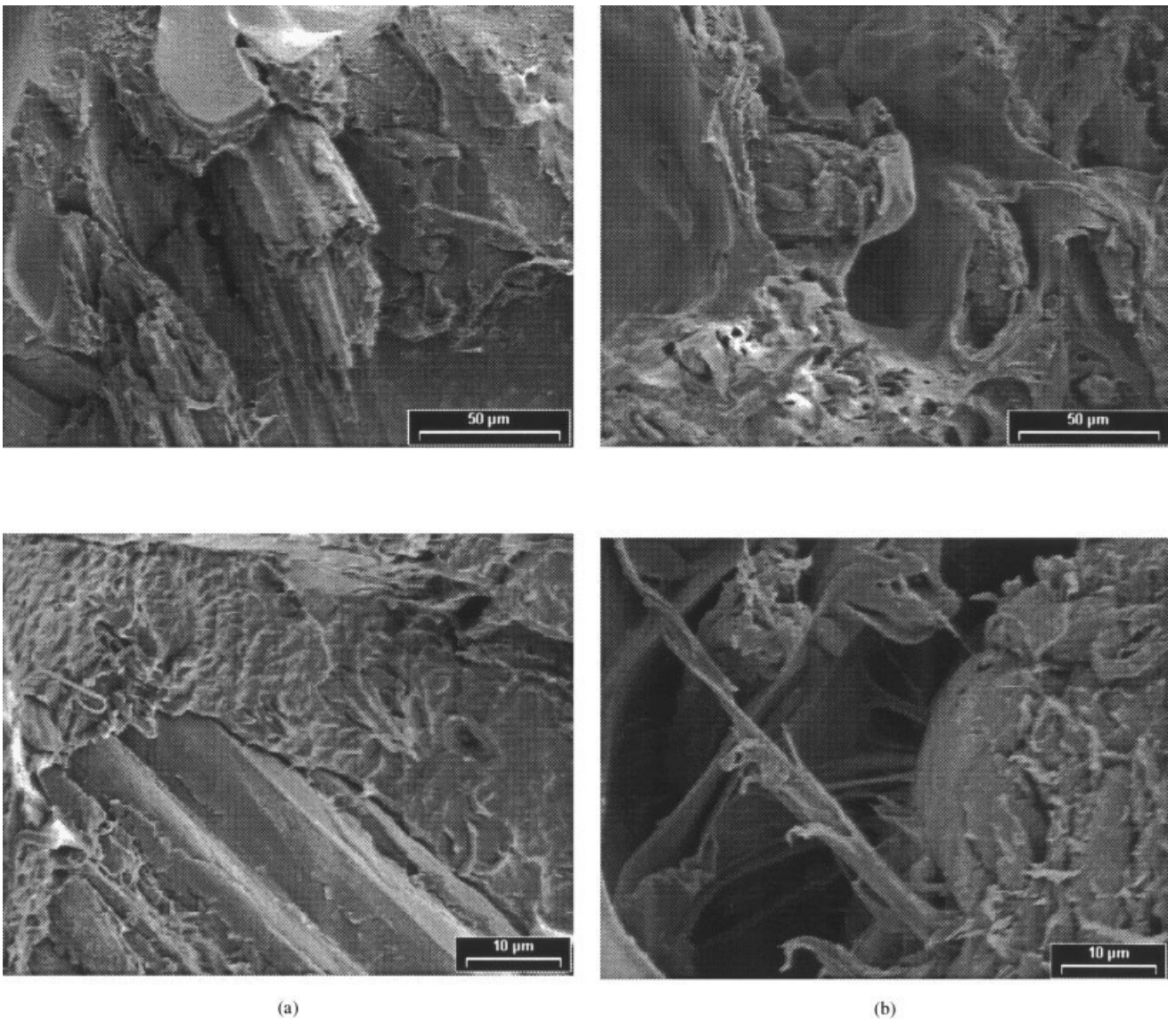

Figure 7 SEM micrographs of the wood flour composites: (a) PEA composites, (b) PEAP composites, and (c) PEAM composites.

Short-term creep tests performed on modified PEs were carried out. Figure 4 shows the behavior of different samples tested at 50°C and 3.2 MPa. The deformation of the PEPM sample is the highest, followed by the strain of the PEP specimen. The unmodified PE exhibits the highest creep resistance. This is the expected behavior because the resistance to deformation increases markedly with X_c in a polymer above its glass–rubber transition temperature.[45] The stability of the molecular state of a crystalline polymer is governed mainly by the crystallinity. Once this is established by a thorough annealing procedure, there is little further change; the temperature of the sample may be changed, as the exigencies of the experimental demand, with little disturbance of the crystallinity, as long as the annealing temperature is not reached. The increased resistance to deformation is accompanied by a decrease in toughness in an impact test and deterioration in the long-term strength.[45]

Short-term creep tests of the composites were also carried out. The effect of the wood flour concentration on the short-term creep response is shown in Figure 5 for PEA composites. The neat polymer shows the highest creep over the whole time range analyzed. The creep resistance of the composites is clearly improved by the addition of wood flour because the creep deformation decreases steadily with an increasing filler concentration. This behavior is expected because Park and Balantinecz[46] demonstrated that the creep of composites made from polypropylene and wood fibers decreases with an increase in Young's modulus. A similar behavior was found when the creep response of PEAP and PEAM composites was analyzed. Composites made from semicrystalline thermoplastics and

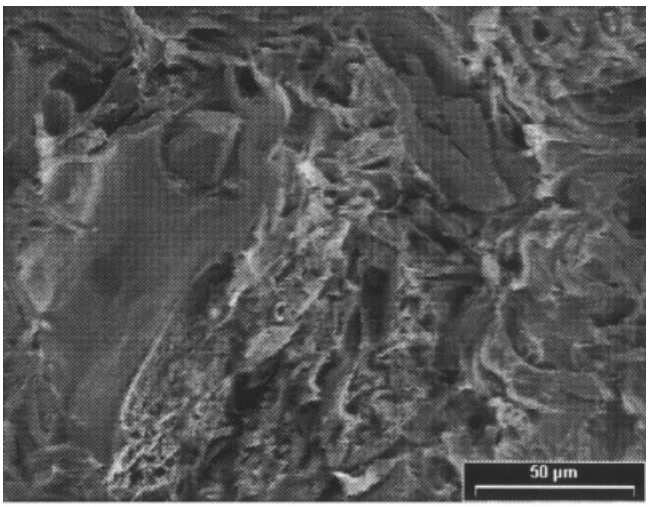

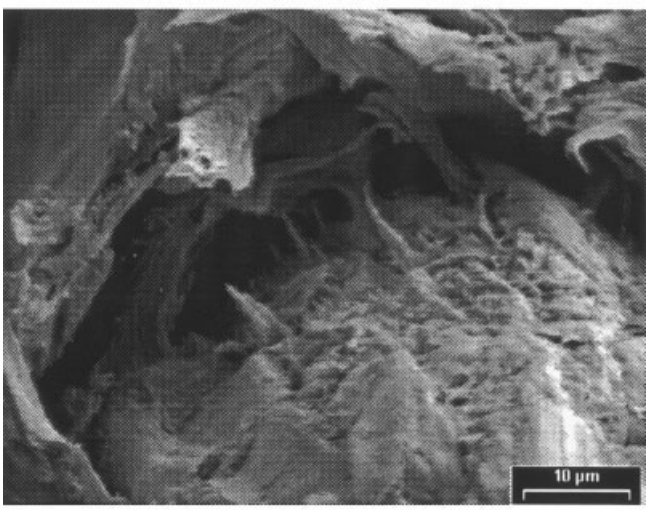

(c)

Figure 7 (*Continued from the previous page*)

rigid fillers show a great variety of mechanical properties that depend on the composition and the processing conditions. The final properties of the composites are governed by the individual properties of the components and by the morphology developed at the matrix/filler interphase. At temperatures higher than the ambient temperature, the mechanical properties of composites with thermoplastic matrices are reduced. However, for composites with higher fiber loadings, this reduction is less pronounced.

The effect of the PE matrix modification on the creep strain of 40 wt % composites is shown in Figure 6. The deformation of the PEAP samples is higher than that of the PEA and PEAM composites. This behavior agrees with an improved dispersion and a better filler–matrix interaction in the PEAM samples. The reduced creep resistance of the PEA and PEAP composites could be attributed to filler particle agglomerates that may be formed because of the reduced compatibility between the polar reinforcement and the nonpolar matrix. For PEAP composites, the lower crystallinity of the PEP matrix (with respect to the unmodified PE) is also responsible for the relatively large creep deformation of their composites.

The four-parameter equation has been used to model the experimental creep deformation. Figures 4–6 show the good agreement between the experimental data and creep curves obtained with eq. (6). Table VI shows the values of the parameters used to model the creep behavior. When a load is applied to a sample, an initial rapid deformation comes from the single spring with the modulus E_1. This is the instantaneous elastic response of the material. Thus, larger values of E_1 will correspond to a more rigid sample behavior, and this parameter follows the same trend as Young's modulus. After this initial deformation, the creep rate decreases rapidly with time (also know as primary creep; see ASTM D 2990), and the deformation is governed by the spring with the modulus E_2 and the dashpot with the viscosity η_2, in parallel. Finally, a steady-state value is reached (also known as secondary creep; see ASTM D 2990), and the deformation in this zone is due to the dashpot with the viscosity η_1. Lower η_1 values correspond to an important contribution of the viscous flow to the total creep. As can be noticed from the values of Table VI, the incorporation of wood flour into the polymeric matrix reduces the viscous flow contribution to the total creep, this reduction being more significant when a stronger filler–matrix interface is obtained. The viscosity of the viscoelastic part of the model, η_1, increases with the wood flour content; for the same filler concentration, with matrix modification, the wood flour acts as a reinforcement, and the reinforcing effect of the wood flour particles is enhanced by the matrix modification.

SEM

Figure 7 shows SEM micrographs taken from the fracture surface of 30 wt % composites. Figure 7(a) (PEA composites) shows more fiber pullout from the matrix during fracture, which suggests weak interfacial shear strength between the filler and the matrix. However, the PE modifications enhance adhesion at the interface, as seen in micrographs from PEAP and PEAM composites. The microstructure of the PEA samples indicates poor interfacial adhesion between the fiber surface and the PE matrix, with no PE matrix coating around the surfaces. There is also a gap between the wood and the PE matrix. However, in the PEAP and PEAM composites, the matrix polymer covers the fiber surfaces. From Figure 7(b) (PEAP composites), it can be seen that the adhered matrix usually ends in quite long strips of material. This result suggests that entanglements formed between the grafted PE and the main PE phase through solubility and interdiffusion

affect a considerable part of the matrix. Figure 7(c) (PEAM composites) shows that there is a large contact area between the matrix and the fiber surface. It is difficult to differentiate the interface of the fibers from the PE matrix.

Finally, air pockets have been observed in almost all the samples, and they lead to porous composites with lower densities and mechanical properties.[21] These are presumably caused when the residual moisture in wood fibers becomes steam during extrusion.

CONCLUSIONS

The properties of composites made from LLDPE reinforced with wood flour have been studied. The results indicate that the final properties can be improved through the modification of the polymer matrix with peroxide and MAn. DSC results indicate that modified PEs are less crystalline than the original material, but the addition of wood flour favors the nucleation process; thus, the X_c values of the composites are higher than those of the corresponding matrix.

PEAP and PEAM composites show moderate and important increments, respectively, in σ_y, ϵ_b (which means an increase in ductility), and toughness with respect to PEA composites, but only PEAM samples show improved creep resistance. The behavior of PEAP composites is related mainly to matrix crosslinking, but the behavior of PEAM composites can be attributed to improved interfacial adhesion. This kind of composite shows improvements in the mechanical properties and performance along with a lower cost of the final material incorporating fibers obtained from renewable sources.

References

1. Rana, A. K.; Mandal, A.; Mitra, B. C.; Jacobson, R.; Rowell, R.; Banerjee, A. N. J Appl Polym Sci 1998, 69, 329.
2. Park, B.-D.; Balantinecz, J. J. J Thermoplast Compos Mater 1996, 9, 342.
3. Balantinecz, J. J.; Woodhams, R. T. Proceedings of Blend and Additives Symposia; Canadian Plastic Institute: Toronto, Canada, 1992; Part 13.
4. Zadorecki, P.; Michell, A. J. Polym Compos 1990, 10, 69.
5. George, J.; Sreekala, M. S.; Thomas, S. Polym Eng Sci 2001, 41, 1471.
6. Glasser, W. G.; Taib, R.; Jain, R. K.; Kander, R. J Appl Polym Sci 1999, 73, 1329.
7. Gauthier, R.; Joly, C.; Coupas, A. C.; Gauthier, H.; Escoubes, M. Polym Compos 1998, 19, 287.
8. Bikiaris, D.; Matzinos, P.; Larena, A.; Flaris, V.; Panayiotou, C. J Appl Polym Sci 2001, 81, 701.
9. Liao, B.; Huang, Y.; Cong, G. J Appl Polym Sci 1997, 66, 1561.
10. Maldas, D.; Kokta, B. V. Int J Polym Mater 1992, 17, 1.
11. Balasuriya, P. W.; Ye, L.; Mai, Y.-W.; Wu, J. J Appl Polym Sci 2002, 83, 2505.
12. Nogellova, Z.; Kokta, B. V.; Chodak, I. J Macromol Sci Pure Appl Chem 1998, 35, 1069.
13. Ahmed, S.; Jones, F. R. J Mater Sci 1990, 25, 4933.
14. Ward, I. M.; Hadley, D. W. An Introduction to the Mechanical Properties of Solid Polymers; Wiley: Chichester, England, 1993; Chapter 8, p 143.
15. Sperling, L. H. Introduction to Physical Polymer Science; Wiley: New York, 1986; Chapter 8, p 367.
16. Mandelkern, L. Crystallization of Polymers; Series in Advanced Chemistry; McGraw-Hill: New York, 1964; Chapter 5.
17. Pérez, C. J.; Cassano, G. A.; Vallés, E. M.; Failla, M. D.; Quinzani, L. M. Polymer 2002, 43, 2711.
18. Rojas de Gáscue, B.; Méndez, B.; Manosalva, J. L.; López, J.; Quiteria, V. R. S.; Müller, A. J. Polymer 2002, 43, 2151.
19. Chartoff, R. P. In Thermal Characterization of Polymeric Materials, 2nd ed.; Turi, E. A., Ed.; Academic: San Diego, 1997; Vol. 1, Chapter 3.
20. Saheb, D. N.; Jog, J. P. Adv Polymer Technol Eng 1999, 18, 351.
21. Nuñez, A. J.; Kenny, J. M.; Reboredo, M. M.; Aranguren, M. I.; Marcovich, N. E. Polym Eng Sci 2002, 42, 733.
22. Sheekala, M. S.; Kumaran, M. G.; Thomas, S. J Appl Polym Sci 1997, 99, 821.
23. Beall, F. C. In Encyclopedia of Materials Science and Engineering, 1st ed.; Bever, M. B., Ed.; Pergamon: Oxford, 1986; Vol. 7.
24. Woodhams, R. T.; Thomas, G.; Rodgers, D. K. Polym Eng Sci 1984, 24, 1166.
25. Rohatgi, P. K.; Satyanarayana, K. G.; Chand, N. In International Encyclopedia of Composites; Lee, S. M., Ed.; VCH: Weinheim, Germany, 1991; Vol. 4.
26. Buttrey, D. N. In Polymer Engineering Composites; Richardson, M. O. W.; Ed.; Applied Science: London, 1977; Chapter 12.
27. Stricker, F.; Bruch, M.; Mülhaupt, R. Polymer 1997, 38, 5347.
28. Bréchet, Y.; Cavaillé, J. Y.; Chabert, E.; Chazeau, L.; Dendievel, R.; Flandin, L.; Gauthier, C. Adv Eng Mater 2001, 3, 571.
29. Marcovich, N. E.; Aranguren, M. I.; Reboredo, M. M. Polymer 2001, 42, 815.
30. Alvarez, V. A.; Valdez, M. E.; Vázquez, A. Polym Test 2003, 22, 611.
31. Pukánszky, B. Composites 1990, 21, 255.
32. Bledzki, A. K.; Gassan, J. Prog Polym Sci 1996, 24, 221.
33. George, J.; Thomas, S.; Bhagawan, S. S. J Thermoplast Compos Mater 1999, 12, 443.
34. Ashby, M. F. Materials Selector in Mechanical Design, 2nd ed.; Butterworth-Heinemann: Oxford, 2000; Chapter 14, p 334.
35. Lundberg, R. D. In Encyclopedia of Polymer Science and Engineering; Kroschwitz, J. I., Ed.; Wiley: New York, 1987; Vol. 8, p 393.
36. Polymer Handbook, 3rd ed.; Brandrup, J.; Immergut, E. H., Eds.; Wiley: New York, 1989; Section V, p 23.
37. Kinloch, A. J.; Young, R. J. Fracture Behavior of Polymers; Applied Science: London, 1983.
38. Kim, J.-K.; Mai, Y.-W. Engineering Interfaces in Fiber Reinforced Composites, 1st ed.; Elsevier: Oxford, 1998; Chapter 6.
39. Folkes, M. J. In Short Fibre Reinforced Thermoplastics; Devis, M. J., Ed.; Wiley: Herts, United Kingdom, 1982.
40. Mascia, L. The Role of Additives in Plastics; Edwar Arnold: London, 1974; Chapter 3.
41. Oksman, K.; Lindberg, H. J Appl Polym Sci 1998, 68, 1845.
42. Rana, A. K.; Mandal, A.; Banerjee, A. N. J Appl Polym Sci 2000, 76, 684.
43. Rozman, H. D.; Kon, B. K.; Abusamah, A.; Kumar, R. N.; Ishak, Z. A. M. J Appl Polym Sci 1998, 69, 1993.
44. Xu, B.; Simonsen, J.; Rochefort, W. E. J Appl Polym Sci 2001, 79, 418.
45. Turner, S. In The Physics of Glassy Polymers, 2nd ed.; Haward, R. N.; Young, R. J., Eds.; Chapman & Hall: London, 1997.
46. Park, B.-D.; Balantinecz, J. J. Polym Compos 1998, 19, 377.
47. Takayanagi, T. M.; Imada, K.; Kajiyama, T. J. Polym Sci Part C 1966, 15, 263.